Proceedings of International Conference on Technology and Social Science 2017
Invited Paper

Experiments on Chaotic Vibrations of a Thin Arch Deformed by an Initial Axial Displacement

Shinichi Maruyama[1, a], Takao Yamaguchi[1,b] and Ken-ichi Nagai[2,c]

[1] Division of Mechanical Science and Technology, Faculty of Science and Technology, Gunma University, 1-5-1 Tenjin-cho, Kiryu, Gunma, 376-8515, JAPAN

[2] Professor Emeritus, Gunma University, 1-5-1 Tenjin-cho, Kiryu, Gunma, 376-8515, JAPAN

[a] maruyama@gunma-u.ac.jp, [b] yamagme3@gunma-u.ac.jp, [c] kennagai@gunma-u.ac.jp

Keywords: nonlinear vibrations, chaotic vibrations, vibrations of continuous body, arch

Abstract. Experimental results are presented on chaotic vibrations of a shallow clamped arch subjected to periodic lateral acceleration. The arch is compressed by an initial axial displacement, then the lowest mode of vibration of the arch has asymmetric form to the mid span. The arch shows characteristics of soften-and-hardening spring involving snap-through transition. Chaotic responses including dynamic snap-through transition and internal resonances are inspected with the maximum Lyapunov exponents, the Fourier spectra and the Poincaré maps. Mode contributions to the chaos are examined with the principal component analysis.

1. Introduction

Thin walled structures are utilized in many vehicles. Arches and beams are fundamental elements of such structures. Since an arch has a curved configuration, the bending stiffness of the arch is much larger than that of a beam. However, when the arch is subjected to lateral load which exceeds a critical magnitude, the arch loses its stability by snap-through buckling. Further, when the arch is excited by a periodic force, then a large amplitude vibration is generated by resonance. In typical regions of the excitation frequency, chaotic responses are abruptly generated. Since nonlinear response of the arch has strong coupling with the axial compressive displacement, the generation of the chaos is affected drastically by the curvature and the axial displacement.

Nonlinear vibrations and chaotic phenomena of arches and beams were studied by many researchers including the authors [1-5]. To reveal the chaotic phenomena of an arch compressed in an axial direction, experimental results are presented of the chaotic vibrations of the arch under periodic acceleration. A thin arch is clamped at both ends and is compressed by the initial axial displacement. Under the periodic lateral acceleration, the chaotic responses of the arch are inspected with the frequency response curves, the maximum Lyapunov exponents, the Fourier spectra and the Poincaré projections. Furthermore, detecting chaotic responses simultaneously at multiple positions of the arch, mode contribution to the chaos is analyzed with the principal component analysis.

2. Test Arch

Fig. 1 shows the test arch fixed on a base frame. A phoshor-bronze arch with thickness h=0.32 mm, breadth b=30 mm and length 280 mm is clamped at the both ends by two rigid blocks on the base frame. The surface of the rigid block is cut to a circular surface. The arch has the effective length L=180 mm and the mean radius R=1.1×104 mm. The arch is painted with acrylic resin of white color. The white surface of the arch is used as a reflection-target of a laser displacement sensor. Material properties are obtained as the Young's modulus E=102 GPa and the mean mass density $\rho=8.9\times10^3$ kg/m^3. Controlling thermal elongations of the arch and the base frame, the initial axial displacement is applied to the arch. Consequently, the arch has larger curvature than that of the mean

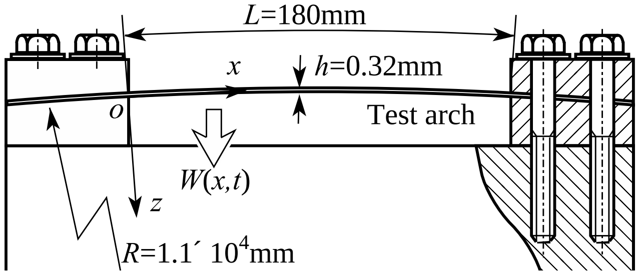

Fig. 1. Test arch

radius R. As shown in the figure, the coordinate system is denoted by x-axis along the arc of the radius R and z-axis in the radial direction. The lateral deflection of the arch is denoted by $W(x,t)$.

3. Vibration Test And Procedure

The following non-dimensional notations are introduced.

$$\xi = x/L,\ w = W/h,\ \alpha = L^2/Rr,\ [p_s, p_d] = [g, a_d](\rho A L^4/EIr),\ q_s = Q_s L^3/EIr,$$
$$\tau = \Omega_0 t,\ [\omega_i, \omega] = [f_i, f](2\pi/\Omega_0),\ \ r = \sqrt{I/A},\ \Omega_0 = L^{-2}\sqrt{EI/\rho A} \qquad (1)$$

Where, r represents the radius of gyration of cross section of the arch, Ω_0 is the coefficient corresponded to lateral vibration of the arch. In Eq. (1), ξ is the non-dimensional coordinate, w is the deflection normalized by the thickness h of the arch. Notation α is the non-dimensional mean curvature of the arch. Notations p_s and p_d are the non-dimensional force intensities related to the gravitational acceleration g and the periodic peak acceleration a_d, respectively. Notations ω and τ are the non-dimensional excitation frequency and the time, respectively. Non-dimensional excitation force is expressed as $p_s+p_d \cos \omega\tau$. When the restoring force of the arch is examined, static deflection under concentrated force Qs is measured. Notation q_s is the non-dimensional concentrated force.

The arch has the mean curvature $\alpha = 32 \pm 2$. The arch is subjected to the static force $p_s = 1.2\times10^3$ due to the gravity. The arch is examined under the amplitude of excitation $p_d = 1.48\times10^3$.

To find the fundamental characteristics of the arch, first, configuration of initial deflection due to the axial displacement and the gravity force on the arch is measured. Next, applying periodic acoustical pressure on the arch, linear natural frequencies are detected with the spectrum analyzer. Finally, the characteristics of the restoring force are examined.

In the vibration test, first, the arch is excited by periodic acceleration with an electromagnetic exciter through the base frame. Next, dynamic time responses of the arch are detected with non-contact laser displacement sensors. Finally, chaotic responses are investigated as following procedure: to find frequency regions where chaotic responses are excited, the nonlinear frequency response curve is inspected. Time progresses of non-periodic responses are examined with the Fourier spectra, the Poincaré projections, the maximum Lyapunov exponents and the principal component analysis. The maximum Lyapunov exponent of the non-periodic response is calculated using the procedure by Wolf et al. [6] and Takens [7]. Recording responses at multiple positions of the arch simultaneously, the principal component analysis [8,9] is applied.

4. Results and Discussion

4.1 Fundamental Characteristics of the Arch

Fig. 2 shows the static initial deflection of the arch measured from the circular arc. The maximum raise of the arc from the line which connects the arch ends is 1.2 times of the arch thickness. The maximum initial deflection is found $\bar{w} = -2.3$ at the mid span of the arch.

Table 1 shows the linear natural frequencies ω_i and the modes of vibration. In the table, the lowest mode of vibration has the asymmetric configuration. This asymmetric form in the vibration is due to the large curvature of the arch. The second mode of vibration shows the symmetric form which is superimposed with the configurations of one half-wave and of three half-waves. Fig. 3 shows the static lateral deflection w of the arch measured at ξ=0.31 under the concentrated force q_s loaded at the mid span of the arch. In the figure, the characteristics of nonlinear restoring force show the type of soften-and-hardening spring including snap-through transition. Without the concentrated force, this arch has two stable equilibrium positions.

4.2 Frequency Response Curves of the Arch

Nonlinear response curves of the arch are recorded under the periodic excitation force $p_d \cos\omega\tau$. The results are shown in Fig. 4. Varying the excitation frequency ω, the dynamic response of the arch at the point ξ=0.31 is recorded by the root mean square value w_{rms}. Notation (i, j) denotes the steady-state periodic response of resonance, in which i is a generated mode of vibration, while j indicates a type of resonance. For example, j =1 indicates the principal resonance, while j =1/2 is the sub-harmonic resonance of 1/2 order. A chaotic response is represented by the notation C(i, j), in which (i, j) corresponds to the dominant mode of vibration and the type of resonance. As the excitation frequency is decreased, resonant responses are generated from the non-resonant responses. When the excitation frequency ω approaches to ω_3 from upper region, the non-resonant steady-state response transits to the other non-resonant response of w_{rms}=4.3. The response involves the static large deflection. At the frequency ω=84.4, the chaotic response C(1,1/2) is generated together with the dynamic snap-through transition from the sub-harmonic resonance (1,1/2). The vibration mode (1,1/2) has the asymmetric form. At the frequency ω=46.5 in the principal resonance of the lowest mode of vibration, chaotic resonance C(1,1) is also generated with the dynamic snap-through. The chaotic response shows non-periodic amplitude variation. At the frequency ω=44.0, the chaotic response jumps to the non-resonant response. In the lower frequency region of the super-harmonic resonance of (2,2), at the frequency ω=37.0, the chaotic response of the type of internal resonance

Table 1. Linear natural frequencies and vibration modes of the arch

Mode number i	Modal pattern	w_i
1	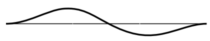	49.2
2	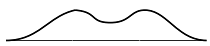	77.1
3		117

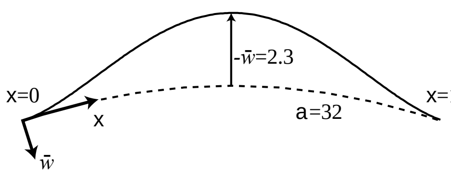

Fig. 2. Configuration of initial deflection of the arch

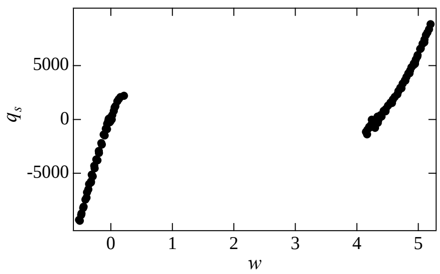

Fig. 3. Static deflection of the arch under concentrated load

C(2,2:3,3) appears. The internal resonance satisfies the condition $\omega_2/2 \approx \omega_3/3$. Furthermore, at ω=35.6, the chaotic response of C(2,2) is excited with the dynamic snap-through. When the excitation frequency is increased continuously from lower frequency region, the chaotic response with the internal resonance C(2,2:3,3) and the chaotic responses with the dynamic snap-through C(1,1) and C(1,1/2) are also generated again.

4.3 Inspection of Chaotic Responses of the Arch

Based on the time progresses of the non-periodic response at ξ=0.31 of the arch, the maximum Lyapunov exponent is calculated by the Wolf's method. Fig. 5 shows the maximum Lyapunov exponents λ_{max} related to the embedding dimension *e* of the chaos of C(2,2:3,3), C(1,1) and C(1,1/2).

In the figure, the maximum Lyapunov exponent of the chaos C(2,2:3,3) takes the value within λ_{max}=1.0 and λ_{max}=1.3 as the embedding dimension exceeds *e*=6. For the chaotic responses of C(1,1) and C(1,1/2), the maximum Lyapunov exponents range from λ_{max}=4.8 to λ_{max}=5.6, near the embedding dimensions exceed *e*=8 or *e*=9. Since the maximum Lyapunov exponents of these responses take the positive values, these responses are confirmed as the chaos. The maximum Lyapunov exponent and the corresponded embedding dimensions of the chaos C(2,2:3,3) with the internal resonance take smaller values than those of the chaotic responses C(1,1) and C(1,1/2). Half of the embedding dimension corresponds to the number of predominant vibration modes that contribute to the chaotic response [3]. Fig. 6 indicates the results of the chaos of the internal resonance C(2,2:3,3) at the frequency ω=38.2. In Fig.6-(a), the time progress of the non-dimensional deflection *w* is presented by the number of excitation period τ_e. The chaotic response vibrates in small amplitudes. Fig. 6-(b) shows the Poincaré projection. In the phase space of the deflection *w* and the velocity $w_{,\omega\tau}$, 6000 points are plotted on the phase delay θ=π/3 from the peak amplitude of the periodic acceleration. The projections within the deflection *w*=0.1 and *w*=0.3 shows the condensed figure, while in the range from *w*=0.4 to *w*=0.7, the projections are focused in band- like strips. The Fourier spectrum of the response is shown in Fig.6-(c). The abscissa represents the non-dimensional Fourier frequency ω_{sp}, while the ordinate stands for the frequency spectra *A* which is scaled by decibel. Dominant spike of spectrum appears at ω_{sp}=76.5 which is twice of the excitation frequency. The response corresponds to the super-harmonic resonance of order two with the second mode of vibration. Furthermore, the peak spike at ω_{sp}=116 corresponds to the super-harmonic resonance of order three related to the third mode. Consequently, the chaotic response is cooperated with the internal resonance which satisfies the relation $\omega_2/2 \approx \omega_3/3$. Fig. 7 shows the chaotic response C(1,1) with the dynamic snap-through. In Fig. 7-(a), the large amplitude time response shows non-periodic behavior. Further, the response transits irregularly around the two stable equilibrium points. In Fig. 7-(b), the Poincaré projections of this response prevails uniformly over the range from *w*=-0.5 to *w*=6. Condensed dotted figure can be observed around *w*=0. From the Fourier spectrum in Fig. 7-(c), predominant peak indicates the response of principal resonance with the lowest mode of vibration.

4.4 Contributions of Vibration Modes to the Chaos of the Arch

The principal component analysis enables one to estimate a contribution ratio of vibration modes in the chaotic response of the arch. The chaotic time progresses of deflection are measured simultaneously at five positions along the arch The modal pattern for the chaos C(2,2:3,3) with the internal resonance is shown in Fig.8(a). The modal patterns φ_i related to the principal component are illustrated in the order of eigenvalue *i*. Contribution ratio is also listed in the figure. The internal resonance is cooperated with the second and third modes of vibration which are symmetric to the mid span of the arch. The largest contribution in the principal components prevails 68%. Its modal pattern corresponds to the second mode of vibration with the symmetric form. The contribution ratio of the third mode to the chaotic response is 2.9%. However, the contribution ratio of the first mode of vibration with the asymmetric form takes 29%. Consequently, for the chaotic response with the

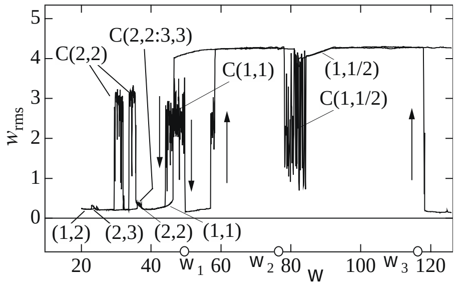

Fig. 4. Frequency response curves of the arch

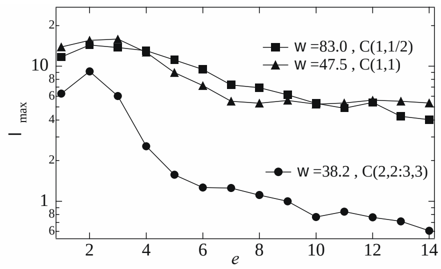

Fig. 5. Maximum Lyapunov exponent related to embedding dimension

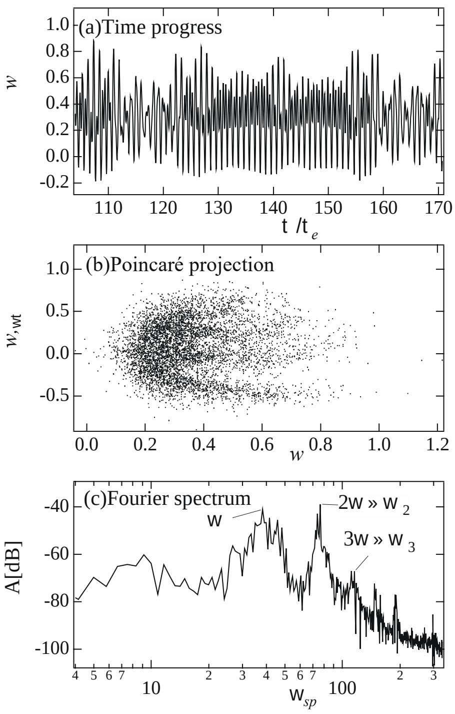

Fig. 6. Chaotic response of the type of C(2,2:3,3), ω=38.2.

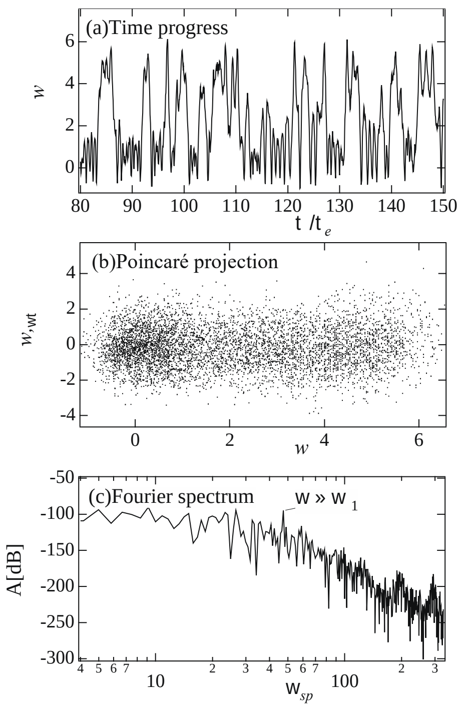

Fig. 7. Chaotic response of the type of C(1,1), ω=47.5.

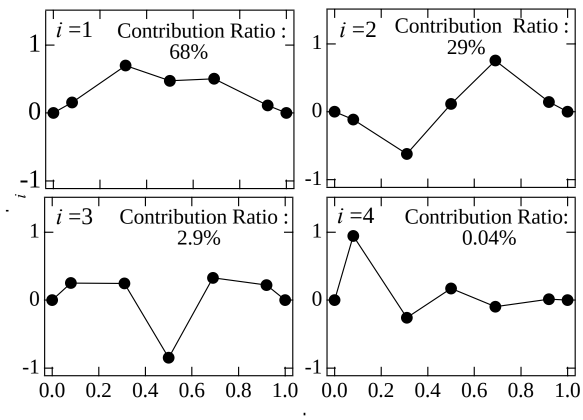

(a) ω=38.2, C(2,2:3,3)

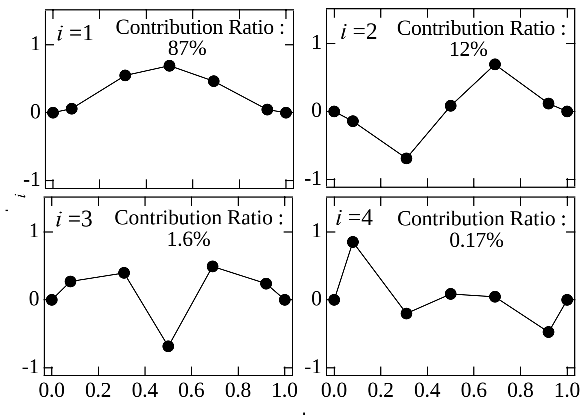

(b) ω=47.5, C(1,1)

Fig. 8. Modal pattern in the chaotic response of the arch obtained by the principal component analysis, ω=38.2, C(2,2:3,3).

internal resonance C(2,2:3,3), the lowest mode of vibration with the asymmetric form have significant contributions to the chaos as well as the second and third modes with the symmetric form.

Fig. 8(b) shows the result of the chaotic response C(1,1) in the principal resonance of the lowest mode having the asymmetric form. The most significant modal pattern is the second mode of vibration with the symmetric form which has contribution ratio of 87%. The response is generated involving the dynamic snap-through. The contribution of the modal pattern with the lowest mode of the asymmetric form has 12%, while the higher modes contribute less than 2%.

5. Conclusion

(1) In the typical frequency region of the internal resonance, the chaotic response is generated in relatively small amplitude. In the sub-harmonic resonance of 1/2 order and the principal resonance corresponded to the lowest mode of vibration, large amplitude chaotic responses appears involving the dynamic snap-through.

(2) In the chaotic response of the internal resonance cooperated with the second and third modes of vibration with the symmetric forms, the lowest mode of vibration with the asymmetric form contributes one-third of the total modes of vibration. When the chaotic response in the type of the dynamic snap-through is generated from the nonlinear periodic resonance, which has the lowest mode with the asymmetric form, the second mode of vibration with the symmetric form has dominant contribution to the chaos.

References

[1] P.J. Holmes, "A nonlinear oscillator with a strange attractor", ***Philo. Trans. of the Royal Soc. London***, Vol. A292, pp. 419-448, 1979.

[2] F.C. Moon and P.J. Holmes, "The magnetoelastic strange attractor", ***J. of Sound and Vib.***, Vol. 65, No. 2, pp. 276-296, 1979.

[3] C. Pezeshki and E.H. Dowell, "Generation and analysis of Lyapunov exponents for the buckled beam", ***Int. J. of Non- Linear Mech.***, Vol. 24, No. 2, pp. 79-97, 1989.

[4] K. Nagai, S. Maruyama, K. Sakaimoto, and T. Yamaguchi, "Experiments on Chaotic Vibrations of a Post-buckled Beam with an Axial Elastic Constraint", ***J. of Sound and Vib.***, Vol. 304, pp. 541-555, 2007.

[5] S. Maruyama, K. Nagai, T. Yamaguchi and K. Hoshi, "Contribution of Multiple Vibration Modes to Chaotic Vibrations of a Post-buckled Beam with an Axial Elastic Constraint", ***Journal of System Design and Dynamics***, Vol. 2, No. 3, pp. 738-749, 2008.

[6] A. Wolf, J.B.Swift, H.L. Swinney and J.A. Vastano, "Determining Lyapunov exponents from a time series", ***Physica***, Vol. 16D, pp. 285-317, 1985.

[7] F. Takens, "Detecting strange attractors in turbulence", ***Lecture Notes in Math.***, D. Rand and L. Young, eds. Springer, New York, Vol.898, pp. 366-381, 1981.

[8] M.M. Loeve, ***Probability Theory***, Princeton NJ, Von Nostrand, 1955.

[9] B.F. Feeny and R. Kappagantu, "On the physical interpretation of proper orthogonal modes in vibrations", ***J. of Sound and Vib.***, Vol. 211, No. 4 , pp. 607-616, 1998.

[10] S. Maruyama, T. Yamaguchi and K. Nagai, " Experiments on Chaotic Vibrations of an Arch Deformed by an Initial Axial Displacement ", ***Journal of Tech. and Social Science***, accepted.